

Microstructure and Mechanical Properties of Vacuum Brazed Nb_{SS}/Nb₅Si₃ Composite Joints Using Ni-Based Filler Alloys



X.Y. REN, H.P. XIONG, Y.W. KANG, C. PEI, B. CHEN, and Y.Y. CHENG

Vacuum brazing of Nb_{SS}/Nb₅Si₃ composite was performed with BNi2 and BNi5 filler alloys at 1293–1423 K for 1800 seconds. The joint microstructures were examined by a scanning electron microstructure (SEM) equipped with an X-ray energy-dispersive spectrometer (XEDS), and shear test for the brazed joints was conducted at room temperature. The Nb_{SS}/Nb₅Si₃ joint brazed with BNi2 filler alloy at 1293 K mainly consisted of Ni₃Si + Nb₃Si, Ni₅Si and borides. As the brazing temperature increased to 1423 K, Cr₂Nb and NbNi phases were formed and the shear strength of the joints was increased from 180 to 253 MPa. Concerning the joints brazed with BNi5 filler at 1423 K, they exhibited an average strength of 274 MPa, and the joint microhardness was lower than BNi2 filler. The BNi5 filler alloy not only raised the shear strength but also decreased the joint brittleness to some extent. As a new finding in this study, 4–5 at. pct Ni had been dissolved into (Nb,Ti)_{SS} in the Nb_{SS}/Nb₅Si₃ composite, providing a new insight into the design of novel specific filler material for Nb_{SS}/Nb₅Si₃ joining.

<https://doi.org/10.1007/s11661-019-05435-2>

© The Minerals, Metals & Materials Society and ASM International 2019

I. INTRODUCTION

WITH the development of aviation industry, severe requirements are put forward for the existing high-temperature structural materials.^[1] To improve the thrust of the turbine system and reduce emissions, higher turbine inlet temperature is demanded, which currently depends on the temperature capacity of turbine blades made of Ni-based superalloys exclusively.^[2,3] However, in general the limited service temperature of the current Ni-based single crystal superalloys is less than 1423 K. Nb_{SS}/Nb₅Si₃ *in situ* composite material is one of the potential high-temperature structural material candidates because of its excellent properties such as high-melting point, low density and attractive high temperature mechanical properties. The potential service temperature of Nb_{SS}/Nb₅Si₃ composite can reach 1473–1673 K and it is very promising to replace the existing nickel-based superalloys.^[4,5] One major drawback of niobium silicides is the low fracture toughness at room temperature, which

seriously restricts its application.^[6] To obtain a high-temperature structural material with balanced mechanical properties including room temperature toughness and high-temperature mechanical strength, dual-phase Nb-Si alloys consisting of the ductile Nb phase and the stiffening Nb₅Si₃ silicide was studied based on the phase diagram.^[7]

Recently, the fabrication techniques and the mechanical properties of Nb_{SS}/Nb₅Si₃ composite have been extensively reported,^[8–13] and the involved techniques include vacuum arc melting,^[7,10] directional solidification,^[6] hot pressing sintering,^[5,9] self-propagating high-temperature synthesis (SHS)^[8] and powder metallurgy technology.^[3]

To realize its practical engineering applications, undoubtedly, joining of Nb_{SS}/Nb₅Si₃ composite will be an extremely important processing technology in future, especially for the aeroengine blades fabricated by Nb_{SS}/Nb₅Si₃ composite with complicated inner cooling tunnels. Due to its high-melting temperature of higher than 1973 K together with the eutectic microstructure of Nb solid solution and Nb₅Si₃ intermetallic compound,^[5] it is difficult to achieve reliable joining of this refractory material. So far, the research on joining technology of Nb_{SS}/Nb₅Si₃ composite and the basic understanding of the joining problem have been seriously lacking.

For the brazing technique, traditional Ni-based filler alloys are widely used for joining of high-temperature structure materials such as stainless steels, Ni-based superalloys including single-crystal superalloys, and even ceramic materials. Recently, Liu *et al.*^[14] investigated the

X.Y. REN, H.P. XIONG, C. PEI, B. CHEN, and Y.Y. CHENG are with the Welding and Plastic Forming Division, Beijing Institute of Aeronautical Materials, Beijing 100095, P.R. China. Contact e-mail: xionghp69@163.com, xionghuaping69@sina.cn Y.W. KANG is with the Science and Technology on Advanced High Temperature Structural Materials Laboratory, Beijing Institute of Aeronautical Materials, Beijing 100095, P.R. China.

Manuscript submitted June 3, 2019.

Article published online August 28, 2019

brazing of GH99 superalloy with BNi2 filler reinforced by graphene. Furthermore, the joining of C_f/SiBCN was conducted with BNi5 filler alloy by Li *et al.*^[15] Based on the binary diagram and thermodynamic principle, element Ni should have a strong affinity with element Nb and form intermetallic compounds. Normally, the Ni-based filler alloy could not be the most appropriate option for Nb_{SS}/Nb₅Si₃ joining. However, it is significant to investigate the effect of elements Ni and Cr on the joining ability of this alloy and to further explore the solubility and permeability of Ni in the Nb_{SS}/Nb₅Si₃ substrates.

In this paper, the primary joining principle of Nb_{SS}/Nb₅Si₃ composites was studied. Joining of Nb_{SS}/Nb₅Si₃ composite was carried out by using two kinds of Ni-based brazing filler alloys (BNi2 and BNi5).^[16] Typical interfacial microstructures and mechanical strength of Nb_{SS}/Nb₅Si₃ joints were analyzed.

II. EXPERIMENTAL

The Nb_{SS}/Nb₅Si₃ *in situ* composite with a nominal composition of Nb-22Ti-16Si-3Cr-3Al-2Hf (at. pct) was used as the parent material, mainly consisting of Nb_{SS}/Nb₅Si₃ eutectic microstructure. The base composite was fabricated by vacuum non-consumable arc melting method and, the ingot was cut into specimens with the size of 13 mm × 13 mm × 5 mm and 13 mm × 13 mm × 3 mm, respectively.

The chemical compositions of BNi2 and BNi5 brazing filler metals are shown in Table I. BNi2 filler metal was fabricated by rapid solidification technique into foils with a thickness of 50 μm. In this study, single foil layer was placed in the gap between the two substrate specimens to form a butt joint, as shown in Figure 1(a). Additionally, BNi5 filler alloy was used in the form of alloying powder (~ 150 mesh).

Prior to the joining procedure, the samples were polished and ultrasonically cleaned with acetone. When using BNi2 filler metal, the brazing experiment was carried out at 1293 K and 1423 K with the brazing time fixed at 1800 seconds. Whereas for BNi5 filler metal, due to its higher liquidus temperature, only 1423 K was chosen as the brazing temperature.

The micro-hardness across the joint section was tested by Vickers indenter (450-SVD) under 50 g, with a fixed loading time of 15 seconds. The hardness value was obtained from at least 3 indentations. The shear strength of the brazed joints was tested at room temperature, as shown in Figure 1(b). The average strength was calculated from four joints. The joint microstructures and the fractured surfaces of the joints were studied using a scanning electron microscope (SEM) equipped with an

X-ray energy-dispersive spectrometer (XEDS). To determine the phase constitution at the fractured surface, an X-ray diffraction (XRD) analysis was also conducted with Cu Kα radiation at 40 kV and 60 mA (D/max-RB, 2θ scanning range between 10 deg and 90 deg).

III. RESULTS AND DISCUSSION

A. Microstructures of the Joints Brazed with BNi2 Filler Alloy

Figure 2 shows backscattered electron images of Nb_{SS}/Nb₅Si₃ joint brazed with BNi2 filler at 1293 K for 1800 seconds, and the corresponding element distribution maps across the joint section are shown in Figure 3. The width of the brazing seam is about 60 μm. During the brazing process, elements Nb and Ti partly diffused from the solid-state Nb-Si substrate into the brazing seam.

The XEDS analysis results in Table II illustrate that the phases at the interface adjacent to the base composite (microzones “1” and “2”) are (Nb,Ti)_{SS} and (Nb,Ti)₅Si₃, respectively. The gray block (microzone “3”) is deduced to be (Nb,Ti)_{SS} dissolved with 18.98 at. pct Ni. Microzones “4” and “9” mainly contain Ni, Si and Nb. Based on the thermodynamic data, the dissolution enthalpy of Si in Nb melt is -173 KJ/mol,^[17] signifying that element Nb has a strong combining capacity with Si. Furthermore, J.S.C. Jang *et al.* conducted the brazing of AISI 304 stainless steel with BNi2 filler metal and the XRD pattern of the fractured joint indicated the formation of four types of phases, that is, Ni solid solution, Ni₃Si, Ni₃B and CrB.^[18] Then, according to the XEDS analyzed results in Table II, microzones “4” and “9” should be the mixture of Ni₃Si + Nb₃Si. In the dark blocks (microzone “5”) and gray matrix (microzone “6”), the Ni content is high up to 74.1 to 79.5 at. pct, indicating the

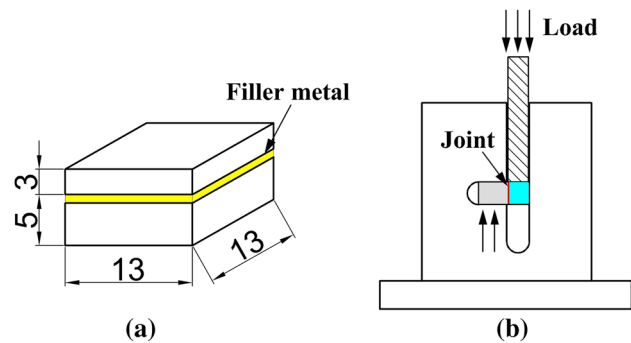


Fig. 1—Illustration of the joint specimen (a) and the shear test (b).

Table I. Composition, Liquidus Temperature and Brazing Temperature of Two Ni-Based Filler Alloys

Filler Alloy	Composition (Mass Fraction, Percent)	Liquidus Temperature (K)	Brazing Temperature (K)
BNi2	Ni-7.0Cr-5.0Si-3.0B-3.0Fe	1272	1293, 1423
BNi5	Ni-19.0Cr-10.0Si	1408	1423

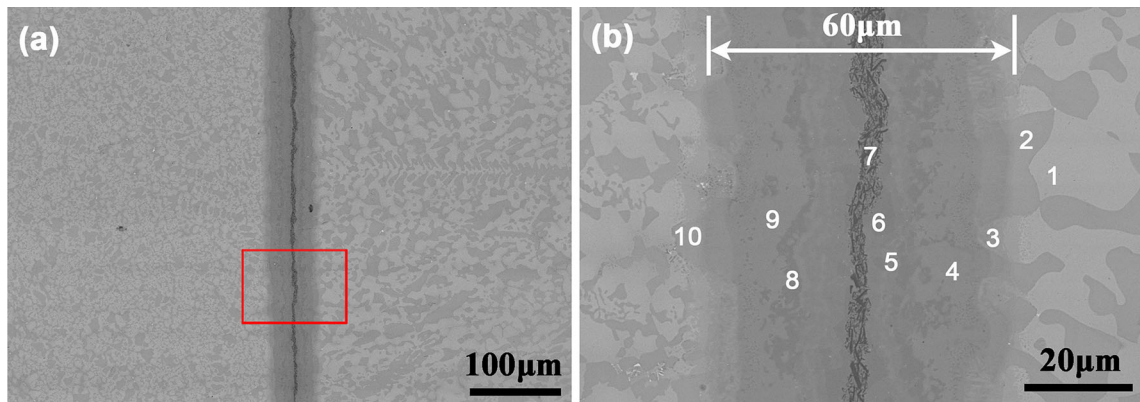


Fig. 2—Backscattered electron image of Nb_{SS}/Nb₅Si₃ joint brazed with BNi2 filler at 1293 K for 1800 s (a), and magnification of the selected area (b).

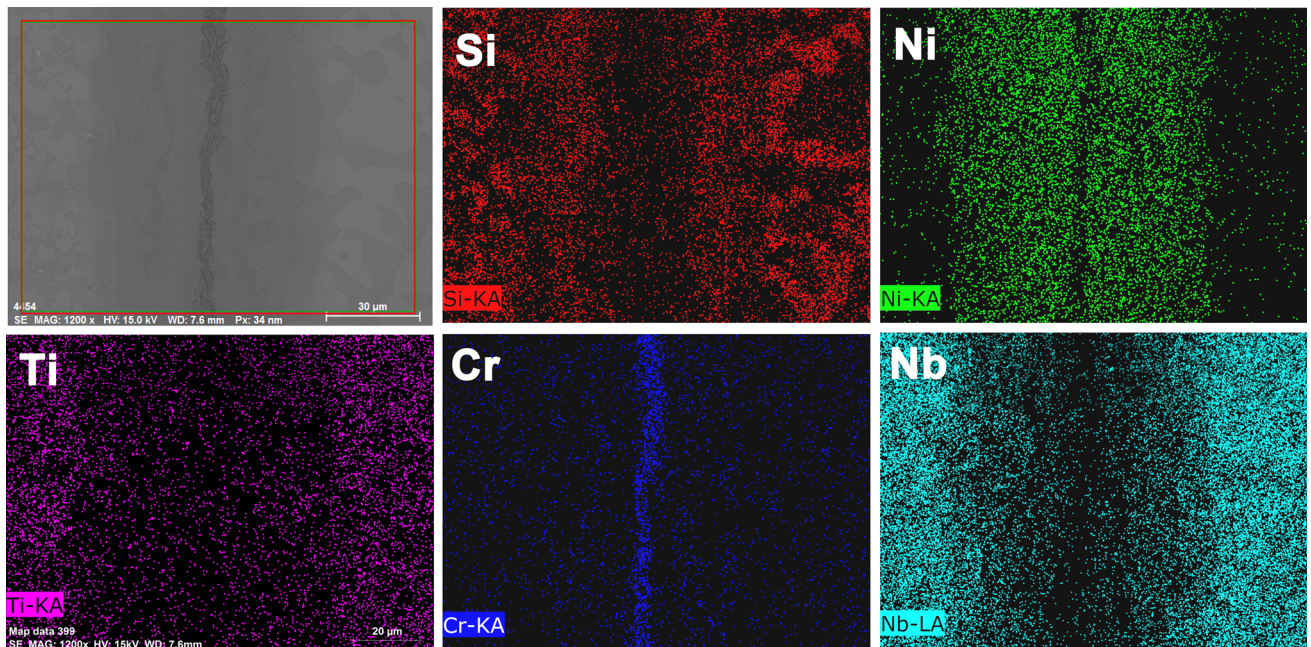


Fig. 3—Microstructure of Nb_{SS}/Nb₅Si₃ joint brazed with BNi2 filler at 1293 K and area distribution maps of elements Si, Ni, Ti, Cr and Nb.

presence of Ni solid solution dissolved with Si, Cr, Ti and Nb. This is also the evidence for that Ti and Nb atoms have partly diffused into the brazing filler alloy. Element Cr is rich in the central part of the brazing seam (Figure 3) and the content of elements Ni and Cr in the dark band (microzone “7”) is 42.2 and 48.3 at. pct, respectively. It is known that the element B is difficult to be detected, and microzone “7” might be boride mixture of Ni₃B and CrB.^[19] Concerning microzone “8”, it is deduced to be Ni₃Si dissolved with Nb, and microzone “10” should be (Nb,Ti)₅Si₃. The Nb_{SS}/Nb₅Si₃ joints brazed with BNi2 filler at 1293 K/1800 s presented an average shear strength of 180 MPa.

Figure 4 presents the microstructure of Nb_{SS}/Nb₅Si₃ joint brazed with BNi2 filler alloy at a higher temperature (1423 K/1800 s). The brazing seam in Figure 4(b) can be divided into three zones. A gray band-like reaction layer is visible on both sides of the brazed seam

(zone “A” and zone “C”). The area distribution maps of elements Cr, Nb, Si, Ti and Ni are shown in Figure 5. The active element Ti and Nb strongly diffused into the brazing seam and the segregation phenomenon of Cr and Nb at some locations was observable in Figure 5.

According to the XEDS analyzed results shown in Table III, the joint matrix in zone “B” (microzone “1”) is composed of Ni₃Si and Nb₃Si, and the XRD peaks in Figure 6(a) further identify their formation within the joint. For microzone “2”, it can be deduced as a mixture of Nb_{SS} and borides. In addition, the XRD peaks associated with the Ni₃B and CrB^[18,19] were indeed detected. The dark phase in microzone “3” should be Cr₂Nb. Moreover, the area distribution of the elements Cr, Si, Ni, and Nb is in good agreement with these deduced phases in Figure 4(b). The microzone “4” can be confirmed as HfO₂^[20] as the atom ratio of O to Hf in this white phase (microzone “4”) is close to 2:1. Evident

Table II. XEDS Analysis Results for the Marked Microzones in Fig. 2(b)

Microzone	Concentration (Atomic Percent)							Deduced Phases
	Nb	Ti	Ni	Si	Al	Cr	Fe	
1	65.20	22.88	/	4.46	3.91	3.55	/	(Nb,Ti) _{SS}
2	43.73	19.75	/	33.60	2.64	0.60	/	(Nb,Ti) ₅ Si ₃
3	63.90	7.19	18.98	6.75	/	3.18	/	(Nb,Ti) _{SS} dissolved with Ni
4	17.15	6.22	52.65	23.98	/	/	/	Ni ₃ Si + Nb ₃ Si
5	1.87	5.48	79.50	4.50	1.35	7.30	/	Ni _{SS}
6	1.80	3.88	74.11	5.19	/	7.97	7.04	borides (Ni ₃ B + CrB)
7	0.87	2.30	42.15	2.46	/	48.33	3.89	Ni ₃ Si dissolved with Nb
8	12.95	5.87	54.59	17.70	/	4.49	4.41	Ni ₃ Si + Nb ₃ Si
9	17.04	5.19	54.22	23.55	/	/	/	(Nb,Ti) ₅ Si ₃
10	45.98	16.64	/	34.26	3.13	/	/	

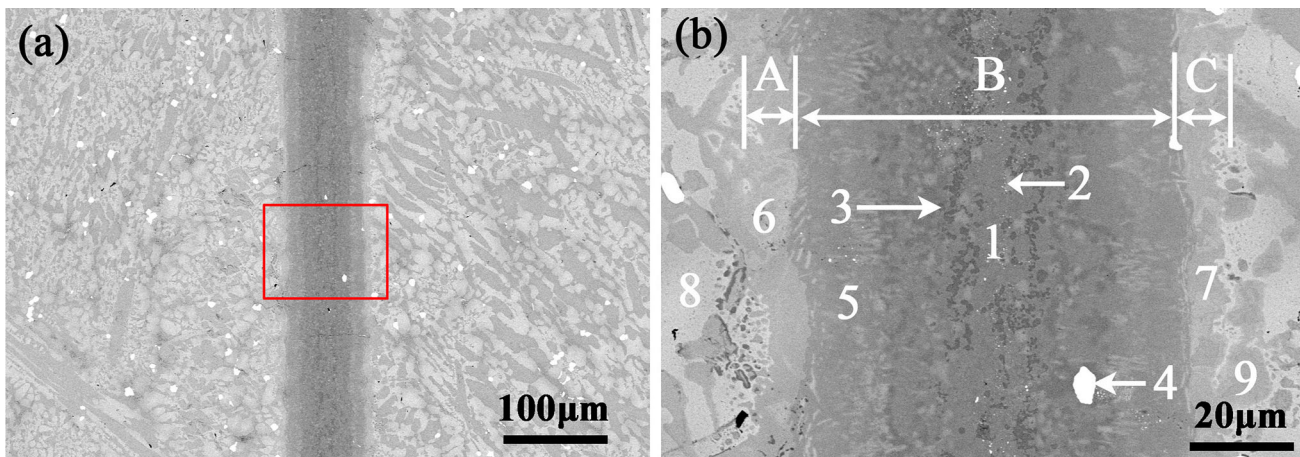
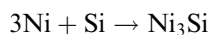
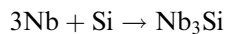
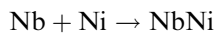
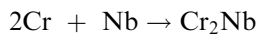


Fig. 4—Backscattered electron image of Nb_{SS}/Nb₅Si₃ joint brazed with BNi2 filler at 1423K (a), and magnification of the selected area (b).

reaction layer (microzones “6” and “7”) is observable at the interface between the brazing seam and the Nb_{SS}/Nb₅Si₃ composite, and they can be deduced to be the mixture of NbNi and (Nb,Ti)_{SS}. Within the surficial layer of the parent material, microzone “8” and “9” should be (Nb,Ti)_{SS} and (Nb,Ti)₅Si₃, respectively.

Therefore, the reaction product sequence of the joint brazed with BNi2 filler at 1423 K for 1800s can be described as (Nb,Ti)_{SS}/(Nb,Ti)₅Si₃ + NbNi + Cr₂Nb + borides + Ni₃Si/Nb₃Si + Cr₂Nb + NbNi + (Nb,Ti)_{SS}/(Nb,Ti)₅Si₃. The main reactions can be summarized by the following expressions:



Compared with the joint brazed at 1293 K, the element diffusion and interface reaction at 1423 K became stronger. During the brazing process, Nb atoms

diffused into the brazing seam strongly and caused the formation of Cr₂Nb. The Nb_{SS}/Nb₅Si₃ joints brazed with BNi2 filler at 1423 K for 1800 seconds exhibited an average shear strength of 253 MPa (Figure 7).

B. Microstructure of Joint Brazed with BNi5 Filler

The backscattered electron images and the corresponding element area distribution maps of Nb_{SS}/Nb₅Si₃ joint brazed with BNi5 filler at 1423 K for 1800 seconds are presented in Figures 8 and 9, respectively. Compared with BNi2 filler, the interfacial microstructure was obviously changed as the element Cr did no longer segregate in the central part of the joint. Meanwhile, the distribution of elements Cr, Si and Ni became more uniform in the brazing seam.

The XEDS analyzed results for the typical microzones are listed in Table IV. In the central area of the brazing seam (Figure 8(b)), the microstructure is characterized by a matrix phase (microzone “1”) and dispersive small dark blocks (microzone “2”), and microzone “1” can be deduced to be (Ni,Cr)₃Si + (Nb,Ti)₃Si.^[21,22] The dark phases (microzone “2”) should be borides. In the case of the black particle (microzone “3”), it is Si-rich phase dissolved with Ni and Cr. Besides, a lamellar structure (microzone “4”) with a thickness of about 10 µm is

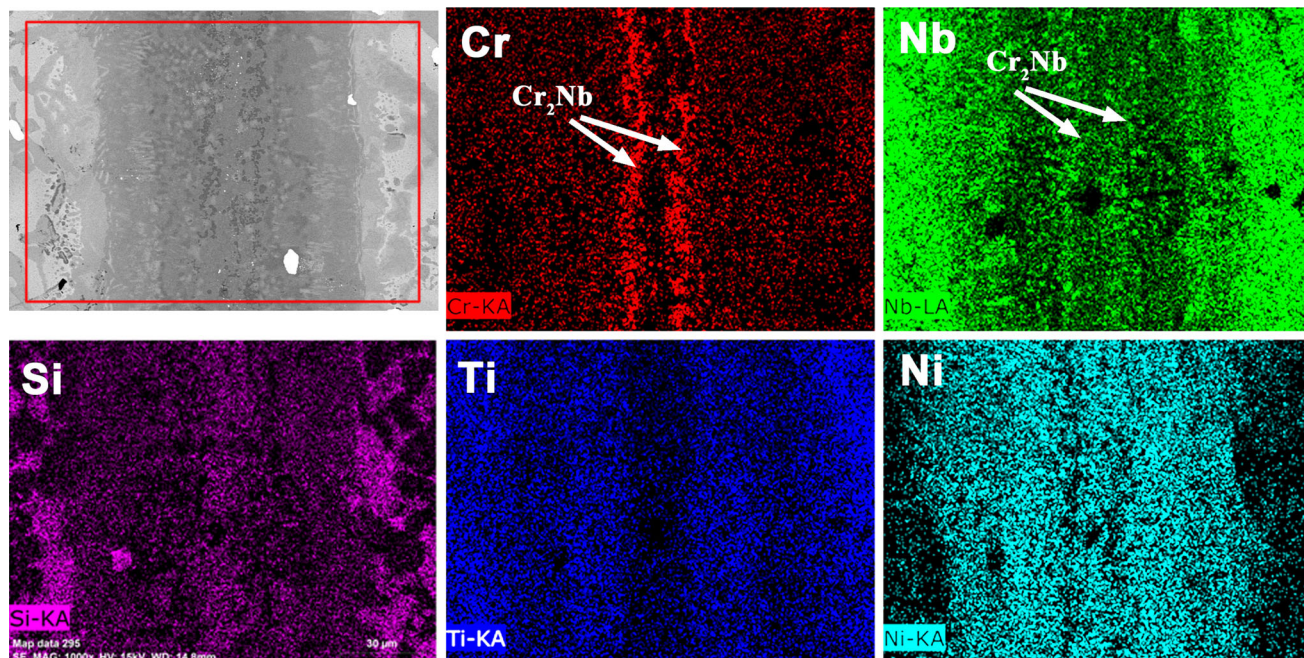


Fig. 5—Microstructure of Nb_{SS}/Nb₅Si₃ joint brazed with BNi2 filler at 1423 K, and element area distribution maps of elements Cr, Nb, Si, Ti and Ni.

Table III. XEDS Analysis Results for the Marked Microzones in Fig. 4(b)

Microzone	Concentration (Atomic Percent)								Deduced Phases
	Nb	Ti	Ni	Si	Al	Cr	Hf	O	
1	18.99	4.05	51.85	25.11	/	/	/	/	Ni ₃ Si + Nb ₃ Si
2	53.48	9.86	17.85	/	/	18.81	/	/	borides + Nb _{SS}
3	33.54	4.98	3.08	0.91	/	57.49	/	/	Cr ₂ Nb
4	/	/	/	/	/	/	37.58	62.42	HfO ₂
5	26.25	10.00	44.60	13.80	/	5.36	/	/	borides + Nb ₅ Si ₃
6	43.74	13.04	33.52	4.08	3.46	2.15	/	/	NbNi + (Nb,Ti) _{SS}
7	40.19	16.14	28.96	6.14	4.89	3.68	/	/	
8	73.69	16.79	/	3.56	3.78	2.18	/	/	(Nb,Ti) _{SS}
9	43.56	19.68	1.77	33.04	1.96	/	/	.	(Nb,Ti) ₅ Si ₃

visible adjacent to Nb_{SS}/Nb₅Si₃ substrate. Figure 9 indicates that this area contains higher Ni and Cr than other areas within the joint, and based on the analyzed results in Table IV it should be the mixture of Ni₃Si + Nb₃Si + CrB. Furthermore, the XRD peaks associated with the three phases are detected in Figure 6(b). In fact, the content of Si (10.0 wt pct) and Cr (19.0 wt pct) in BNi5 is much higher than BNi2. Therefore, both Ni₃Si and CrB could be easily formed during the brazing process.^[23,24] The gray (Nb,Ti)₅Si₃ phase (microzone “5”) and white (Nb,Ti)_{SS} phase dissolved with 4.41 at pct Ni (microzone “6”) are observed in the Nb_{SS}/Nb₅Si₃ substrate area. The joints brazed with BNi5 filler at 1423 K for 1800 seconds presented an average shear strength of 274 MPa (Figure 7).

It should be pointed out that when joined with BNi5 brazing filler, Cr₂Nb phase was not detected within the

brazing seam despite the higher Cr content in BNi5. As presented in Figure 10, considering the high content of Si (10.3 wt pct) in BNi5, the Nb₃Si compound was *in situ* formed by the reaction of Si and Nb atoms from the substrate material. The dissolution enthalpy of element Nb in melts of Cr and Si is – 35 and – 173 KJ/mol, respectively.^[17] Hence, Nb-Si compound should be more easily to form in the brazing seam during the interfacial reaction than Cr-Nb compound. Nb atoms from the substrates had reacted with Si before it could diffuse to the center of the brazing seam. Thus Cr₂Nb compound was absent in the BNi5 brazed joint. According to the Nb-Si binary phase diagram, as a refractory compound Nb₃Si phase exhibits a high-melting point of about 2218-2248 K.^[25,26] To some extent, the presence of Nb₃Si within the brazing seam should be favorable to the high-temperature joint

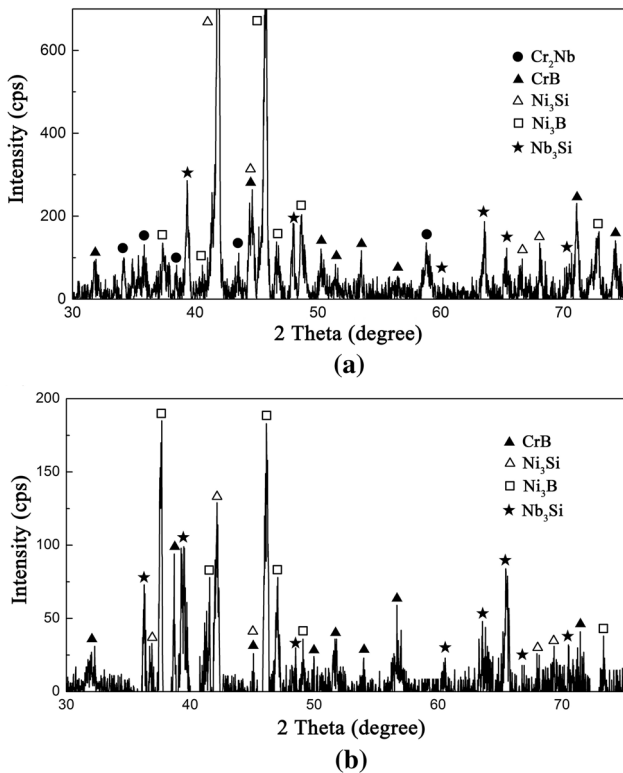


Fig. 6—XRD pattern of the fracture surface of joints brazed with: (a) BNi2 filler alloy, 1423 K/1800 s; (b) BNi5 filler alloy, 1423 K/1800 s.

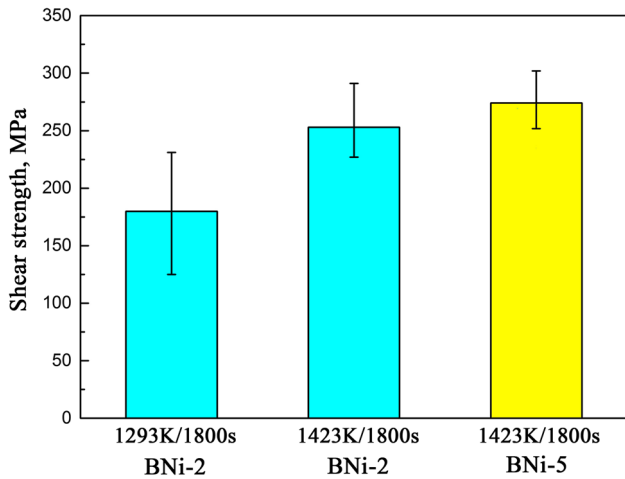


Fig. 7—Shear strength of three kinds of joints: BNi2 joint brazed at 1293 K and 1423 K for 1800 s, and BNi5 joint brazed at 1423 K for 1800 s.

strength. Borides were detected in the brazing seam of the joints brazed with both BNi2 and BNi5 filler alloys. Furthermore, coupled with the XEDS results, element Ni could diffuse into the Nb-Si substrate material and could be dissolved into the (Nb,Ti)_{SS} with about 4-5 at. pct concentration (Figure 10(d)). This phenomenon could provide a new insight into the design of novel filler alloy for Nb_{SS}/Nb₅Si₃ joining in future.

C. Mechanical Properties of Nb_{SS}/Nb₅Si₃ Joints

The micro-hardness profiles along the cross-section of the two kinds of brazed joints are displayed in Figure 11. In general, the hardness values within the brazing seams are higher than the base materials. In the case of BNi2 fillers (Figure 11(a)), the maximum hardness of 1240 HV appears within the central part of the brazing seam (microzone “1”). As described previously, the phase in the central part is deduced to be a mixture of Ni₃Si and Nb₃Si. It was reported that the Vickers hardness of Nb₃Si in Nb-22Ti-16Si-4Zr was high up to 1157 HV.^[27] Therefore, owing to the formation of Ni₃Si and Nb₃Si intermetallic compounds,^[28–30] microzone “1” presented a high-micro-hardness. Microzone “2” in Figure 4(b), mainly composed of Nb_{SS} + borides, exhibits significantly lower micro-hardness value of about 490 HV. As a Laves-type intermetallic compound, Cr₂Nb phase is considered to be brittle at low temperatures for its complex crystal structure and limited operative slip systems available for deformation, with a melting point of 2043 K.^[31] In microzone “3”, the presence of the Cr₂Nb makes the micro-hardness at the level of about 1150 HV. Moreover, the micro-hardness in the Nb_{SS}/Nb₅Si₃ substrate area is about 480 HV.

With respect to the joints brazed with BNi5 filler, the micro-hardness profile (Figure 11(b)) shows a different variation trend. From the substrate material to the brazing seam, the micro-hardness value first rises steeply and then falls down. The maximum micro-hardness (970 HV) occurs in the lamellar structure (microzone “4” in Figure 8(b)) mainly consisting of Ni₃Si + Nb₃Si + CrB. Correspondingly, the matrix phases in the central area of the brazed seam, with the mixture of (Ni,Cr)₃Si + (Nb,Ti)₃Si and borides, present a lower micro-hardness of about 700 HV. Similar to the joint brazed with BNi2 filler, the micro-hardness of substrate area is 480-490 HV.

The average shear strength of Nb_{SS}/Nb₅Si₃ joints brazed with BNi2 filler alloy at 1293 K and 1423 K for 1800 seconds are 180 and 253 MPa, respectively. With regard to the BNi5 filler, the joints brazed at 1423 K for 1800 seconds present an increased shear strength of 274 MPa (Figure 7).

Further analysis for the fractured surface of the joints after the shear test was conducted. The backscattered electron images of the two fractured surfaces reveal that both the fracture behaviors should be identified as brittle fracture.^[32] Figure 12(a) shows the fractured surface of the Nb_{SS}/Nb₅Si₃ joints brazed with BNi2 filler alloy at 1423 K for 1800 seconds. The fracture mainly occurred along the Ni₃Si, Nb₃Si and borides (Ni₃B + CrB) phases in the central area of the brazing seam (microzones “1” and “2” in Figure 4(b)). In general, the formation of brittle intermetallics in the brazing seam could decrease the joint strength.^[33] Evidently, due to the high-micro-hardness, the mixture of Ni₃Si and Nb₃Si phases would be detrimental to the joint strength.^[34] As a consequence, brittle fracture occurred quickly in this area when the shear stress was loaded during the shear test.

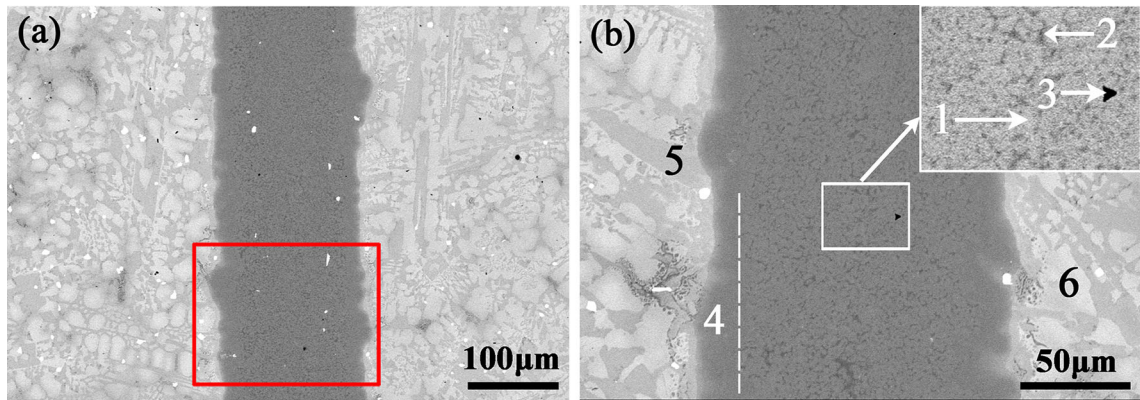


Fig. 8—Microstructure of Nb_{SS}/Nb₅Si₃ joint brazed with BNi5 filler at 1423 K/1800 s (a), and magnification of the selected area (b).

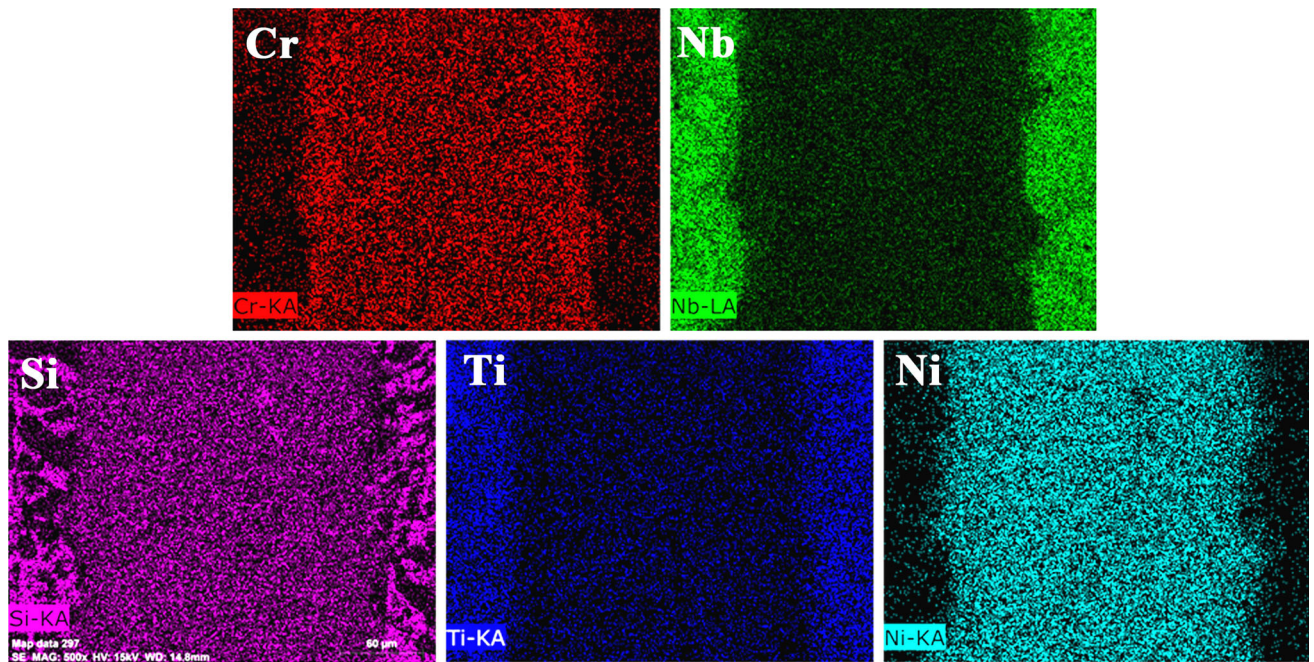


Fig. 9—Area distribution maps of elements: Cr, Nb, Si, Ti and Ni for Fig. 8(b).

Table IV. XEDS Analysis Results for the Marked Microzones in Fig. 8(b)

Microzone	Concentration (Atomic Percent)								Deduced Phases
	Nb	Ti	Ni	Si	Al	Cr	Hf	O	
1	10.63	5.56	53.12	24.66	/	6.03	/	/	(Ni,Cr) ₃ Si + (Nb,Ti) ₃ Si
2	/	/	55.63	10.47	/	33.90	/	/	borides (Ni ₃ B + CrB)
3	5.94	3.14	31.21	50.05	/	9.67	/	/	Si-rich phase
4	12.42	2.37	46.25	19.37	/	19.59	/	/	Ni ₃ Si + Nb ₃ Si + CrB
5	47.06	14.58	0.15	38.21	/	/	/	/	(Nb,Ti) ₅ Si ₃
6	73.51	20.40	4.41	1.68	/	/	/	/	(Nb,Ti) _{SS}

The fractured surface of the Nb_{SS}/Nb₅Si₃ joints brazed with BNi5 filler at 1423 K for 1800 seconds is shown in Figure 12(b). Ni₃Si and Nb₃Si are detected by XEDS and XRD. The (Nb,Ti)_{SS} in substrate area is also visible. Hence, the crack mainly propagated along the reaction zone (microzone “4” in Figure 8(b))

between the substrate and the brazing seam. Furthermore, the overall micro-hardness of the joint brazed with BNi5 (Figure 11(b)) was generally lower than that in Figure 11(a), indicating that the BNi5 filler alloy, to some extent, not only improved the joint strength but also decreased the joint brittleness. As

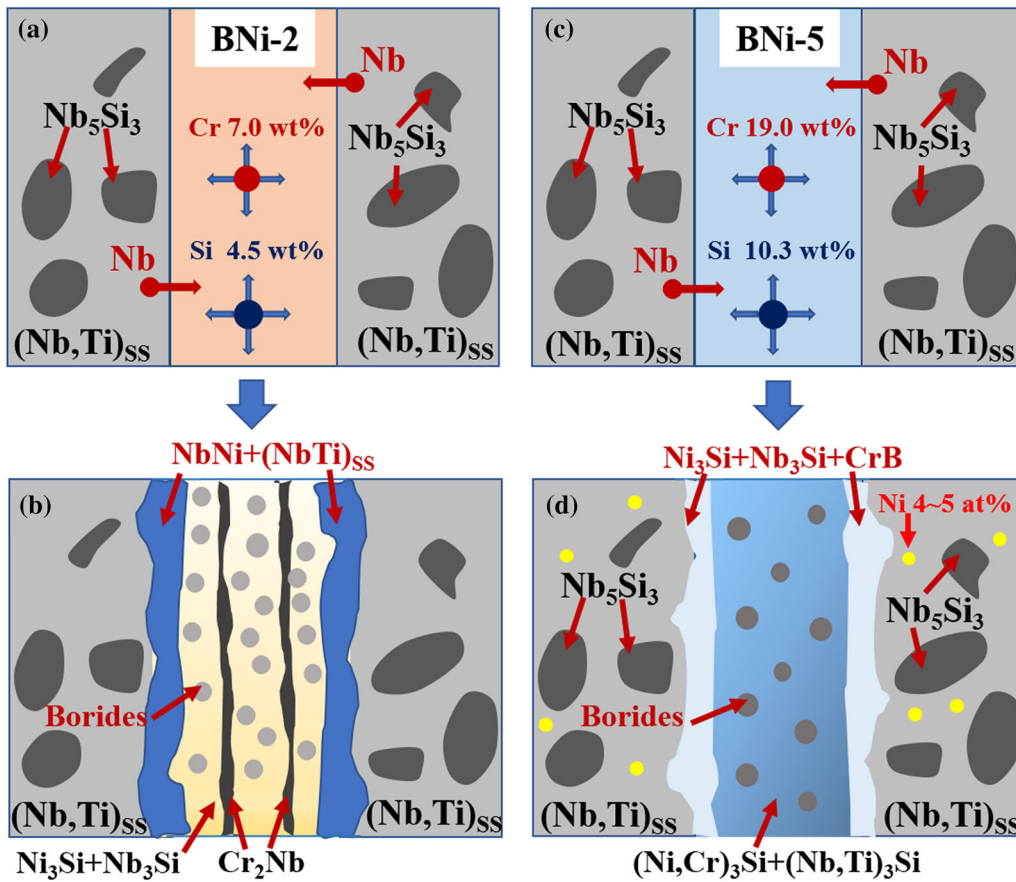


Fig. 10—Interface evolution model of the $\text{Nb}_{\text{SS}}/\text{Nb}_5\text{Si}_3$ joints brazed with BNi2 filler (a, b), and BNi5 filler (c, d).

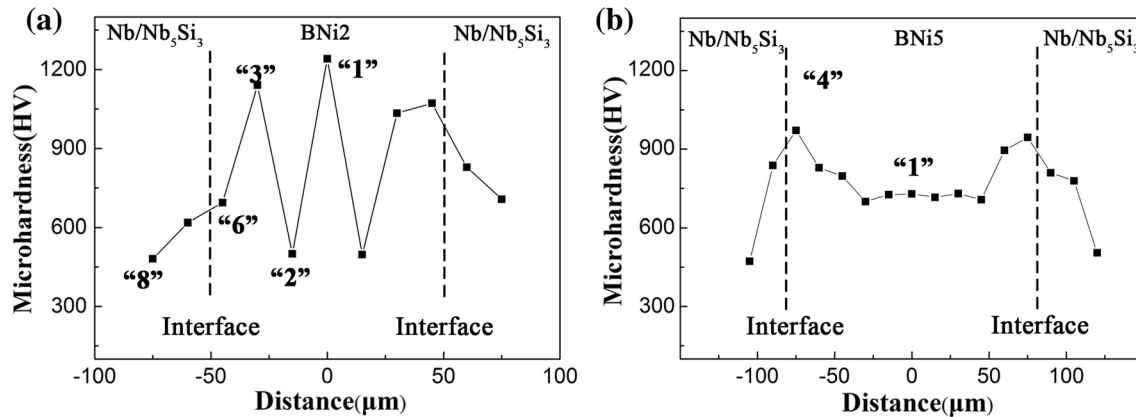


Fig. 11—Vickers hardness of the $\text{Nb}_{\text{SS}}/\text{Nb}_5\text{Si}_3$ joints brazed with: (a) BNi2 filler, 1423 K/1800 s (Fig. 4(b)); (b) BNi5 filler, 1423 K/1800 s (Fig. 8(b)).

another important finding in this study, 4-5 at. pct Ni could be dissolved into the (Nb, Ti) solid solution phase in the Nb-Si substrate material, which could offer a new idea for the composition design of the novel filler alloy for $\text{Nb}_{\text{SS}}/\text{Nb}_5\text{Si}_3$ composite joining. With the progress of the research on the composition optimization of $\text{Nb}_{\text{SS}}/\text{Nb}_5\text{Si}_3$ composites and their fabrication technique,^[7,10,13,35] it is highly needed for the study of novel filler alloys, in which element Ni

frequently should be an effective melting point depressant element.

IV. CONCLUSIONS

Two kinds of Ni-based fillers, BNi2 and BNi5, were chosen as filler alloy for $\text{Nb}_{\text{SS}}/\text{Nb}_5\text{Si}_3$ composite joining. Main conclusions are summarized as follows:

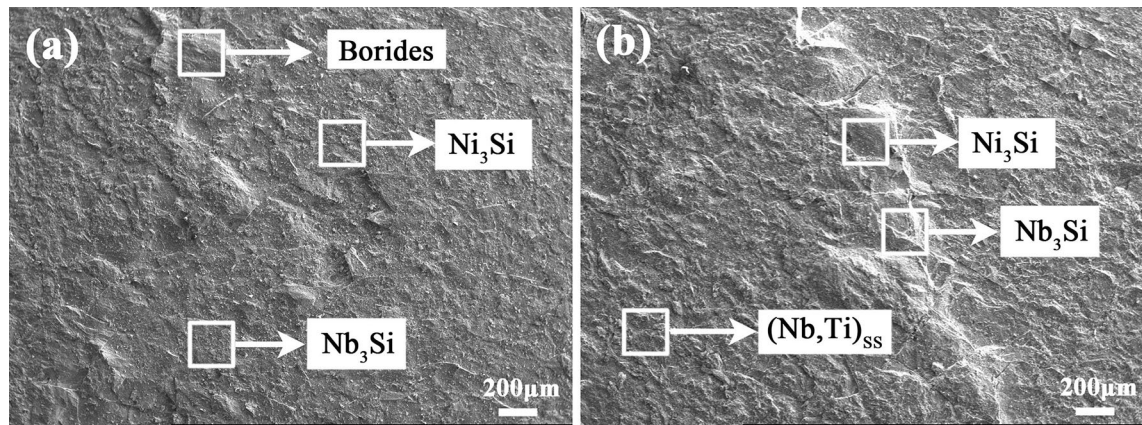


Fig. 12—Fractured surface of two kinds of joints: (a) BNi2 joint, 1423 K/1800 s; (b) BNi5 joint, 1423 K/1800 s.

- (1) The Nb_{SS}/Nb₅Si₃ joint brazed with BNi2 filler alloy at 1093 K mainly consisted of Ni₃Si + Nb₃Si, Ni_{SS} and borides. The overall phase sequence of the joint brazed with BNi2 filler at 1423 K can be described as (Nb,Ti)_{SS}/(Nb,Ti)₅Si₃ + NbNi + Cr₂Nb + borides + Ni₃Si/Nb₃Si + Cr₂Nb + NbNi + (Nb,Ti)_{SS}/(Nb,Ti)₅Si₃.
- (2) While using BNi2 filler alloy, as the brazing temperature increased to 1423 K, the interface reaction became more sufficient and the shear strength increased from 180 to 253 MPa.
- (3) When brazed with BNi5 filler alloy, element Ni could diffuse and be dissolved into (Nb,Ti)_{SS} substrate area with 4-5 at. pct concentration, providing a new insight into the design of novel filler alloy for Nb_{SS}/Nb₅Si₃ joining in future.
- (4) For the joints brazed with BNi5 filler alloy, the reaction products mainly consisted of Ni₃Si, Nb₃Si and borides. The joint exhibited a lower micro-hardness than BNi2 filler and the average shear strength reached 274 MPa. To some extent, BNi5 filler alloy not only raised the shear strength but also decreased the joint brittleness.

REFERENCES

1. B.P. Bewlay, J.J. Lewandowski, and M.R. Jackson: *JOM*, 1997, vol. 49, pp. 44–45.
2. B.P. Bewlay, M.R. Jackson, J.C. Zhao, P.R. Subramanian, M.G. Mendiratta, and J.J. Lewandowski: *MRS Bull.*, 2003, vol. 28, pp. 646–53.
3. J.H. Kim, T. Tabaru, M. Sakamoto, and S. Hanada: *Mater. Sci. Eng. A*, 2004, vol. 372, pp. 137–44.
4. F. Gang, A. Kauffmann, and M. Heilmaier: *Metall. Mater. Trans. A*, 2018, vol. 49A, pp. 763–71.
5. W. Liu, H.P. Xiong, N. Li, S.Q. Guo, and R.Y. Qin: *Acta Metall. Sin. (Engl. Lett.)*, 2018, vol. 31, pp. 362–70.
6. Y.W. Kang, Y.C. Yan, J.X. Song, and H.S. Ding: *Mater. Sci. Eng. A*, 2014, vol. 599, pp. 87–91.
7. Y. Tang and X. Guo: *Metall. Mater. Trans. A*, 2018, vol. 49A, pp. 4884–94.
8. C.L. Yeh and W.H. Chen: *J. Alloys Compd.*, 2005, vol. 402, pp. 118–23.
9. J.L. Yu, K.F. Zhang, Z.K. Li, X. Zheng, G.F. Wang, and R. Bai: *Scr. Mater.*, 2009, vol. 61, pp. 620–23.
10. Y.W. Kang, S.Y. Qu, J.X. Song, Q. Huang, and Y.F. Han: *Mater. Sci. Eng. A*, 2012, vol. 534, pp. 323–28.
11. G.M. Cheng, Y.X. Tian, L.L. He, and J.T. Guo: *Philos. Mag.*, 2009, vol. 89, pp. 2801–12.
12. J.L. Yu and K.F. Zhang: *Scr. Mater.*, 2008, vol. 59, pp. 714–17.
13. L.N. Jia and H. Zhang: *Metall. Mater. Trans. A*, 2018, vol. 49A, pp. 1295–1303.
14. D. Liu, Y.Y. Song, B. Shi, Q. Zhang, X.G. Song, H.W. Niu, and J.C. Feng: *J. Mater. Sci. Technol.*, 2018, vol. 34, pp. 1843–50.
15. W.W. Li, B. Chen, Y. Xiong, H.P. Xiong, Y.Y. Cheng, and W.J. Zou: *J. Mater. Sci. Technol.*, 2017, vol. 5, pp. 487–91.
16. R.F. Li, Z.S. Yu, and K. Qi: *Adv. Mater. Res.*, 2013, vol. 602, pp. 2087–91.
17. A.R. Miedema, F.R. De Boer, and R. Boom: *Calphad*, 1977, vol. 1, pp. 341–59.
18. J.S.C. Jang and H.P. Shih: *J. Mater. Sci. Lett.*, 2003, vol. 22, pp. 79–82.
19. J. Ruiz-Vargas, N. Siredey-Schwaller, N. Gey, P. Bocher, and A. Hazotte: *J. Mater. Process. Technol.*, 2013, vol. 213, pp. 20–29.
20. J. Geng, P. Tsakiroopoulos, and G.S. Shao: *Intermetallics*, 2007, vol. 15, pp. 69–76.
21. X.J. Yuan, C.Y. Kang, and M.B. Kim: *Mater. Charact.*, 2009, vol. 60, pp. 923–31.
22. M.A. Arafin, M. Medraj, D.P. Turner, and P. Bocher: *Mater. Chem. Phys.*, 2017, vol. 106, pp. 109–19.
23. M.A. Arafin, M. Medraj, D.P. Turner, and P. Bocher: *Mater. Sci. Eng. A*, 2007, vol. 447, pp. 125–33.
24. Z. Chen and Y.W. Yan: *J. Alloys Compd.*, 2006, vol. 413, pp. 73–76.
25. Y. Luo, W.C. Jiang, Y.C. Zhang, M.M. Hao, and S.T. Tu: *Mater. Sci. Eng. A*, 2018, vol. 711, pp. 223–32.
26. D.K. Deardorff, R.E. Siemens, P.A. Romans, and R.A. McCune: *J. Less-Common Met.*, 1969, vol. 18, pp. 11–26.
27. Y.X. Tian, J.T. Guo, L.Y. Sheng, G.M. Cheng, L.Z. Zhou, L.L. He, and H.Q. Ye: *Intermetallics*, 2008, vol. 16, pp. 807–12.
28. M.M. Verdian, K. Raeissi, and M. Salehi: *Appl. Surf. Sci.*, 2012, vol. 261, pp. 493–98.
29. S. Milenkovic and R. Caram: *J. Cryst. Growth*, 2002, vol. 237, pp. 95–100.
30. V. Jalilvand, H. Omidvar, H.R. Shakeri, and M.R. Rahimpour: *Mater. Charact.*, 2013, vol. 75, pp. 20–28.
31. G.E. Vignoul, J.K. Tien, and J.M. Sanchez: *Mater. Sci. Eng. A*, 1993, vol. 170, pp. 177–83.

32. J. Chen, V. Demers, D.P. Turner, and P. Bocher: *Metall. Mater. Trans. A*, 2018, vol. 49, pp. 1244–53.
33. H.S. Furuya, Y.S. Sato, H. Kokawa, T. Huang, and R.S. Xiao: *Metall. Mater. Trans. A*, 2018, vol. 49A, pp. 6215–23.
34. H.S. Ren, H.P. Xiong, B. Chen, S.J. Pang, B.Q. Chen, and L. Ye: *J. Mater. Sci. Technol.*, 2016, vol. 32, pp. 372–80.
35. N. Li, S. Huang, G.D. Zhang, R.Y. Qin, W. Liu, H.P. Xiong, G.Q. Shi, and J. Blackburn: *J. Mater. Sci. Technol.*, 2019, vol. 35, pp. 242–69.

Publisher's Note Springer Nature remains neutral with regard to jurisdictional claims in published maps and institutional affiliations.